Physics Letters B 781 (2018) 735–740

Contents lists available at ScienceDirect

Physics Letters B

www.elsevier.com/locate/physletb

Σ^0 production in proton nucleus collisions near threshold

HADES Collaboration

J. Adamczewski-Musch [d], G. Agakishiev [g], O. Arnold [i,j], E.T. Atomssa [o], C. Behnke [h], J.C. Berger-Chen [i,j], J. Biernat [c], A. Blanco [b], C. Blume [h], M. Böhmer [j], P. Bordalo [b], S. Chernenko [g], C. Deveaux [k], A. Dybczak [c], E. Epple [i,j], L. Fabbietti [i,j,*], O. Fateev [g], P. Fonte [b,1], C. Franco [b], J. Friese [j], I. Fröhlich [h], T. Galatyuk [e,2], J.A. Garzón [q], R. Gernhäuser [j], K. Gill [h], M. Golubeva [l], F. Guber [l], M. Gumberidze [e,2], S. Harabasz [c,e], T. Hennino [o], S. Hlavac [a], C. Höhne [k], R. Holzmann [d], A. Ierusalimov [g], A. Ivashkin [l], M. Jurkovic [j], B. Kämpfer [f,3], T. Karavicheva [l], B. Kardan [h], I. Koenig [d], W. Koenig [d], B.W. Kolb [d], G. Korcyl [c], G. Kornakov [e], R. Kotte [f], A. Krása [p], E. Krebs [h], H. Kuc [c,o], A. Kugler [p], T. Kunz [j,*], A. Kurepin [l], A. Kurilkin [g], P. Kurilkin [g], V. Ladygin [g], R. Lalik [i,j], K. Lapidus [i,j], A. Lebedev [m], L. Lopes [b], M. Lorenz [h], T. Mahmoud [k], L. Maier [j], S. Maurus [i,j], A. Mangiarotti [b], J. Markert [h], V. Metag [k], J. Michel [h], C. Müntz [h], R. Münzer [i,j], L. Naumann [f], M. Palka [c], Y. Parpottas [n,4], V. Pechenov [d], O. Pechenova [h], V. Petousis [n], J. Pietraszko [d], W. Przygoda [c], S. Ramos [b], B. Ramstein [o], L. Rehnisch [h], A. Reshetin [l], A. Rost [e], A. Rustamov [h], A. Sadovsky [l], P. Salabura [c], T. Scheib [h], K. Schmidt-Sommerfeld [j], H. Schuldes [h], P. Sellheim [h], J. Siebenson [j], L. Silva [b], Yu.G. Sobolev [p], S. Spataro [5], H. Ströbele [h], J. Stroth [h,d], P. Strzempek [c], C. Sturm [d], O. Svoboda [p], A. Tarantola [h], K. Teilab [h], P. Tlusty [p], M. Traxler [d], H. Tsertos [n], T. Vasiliev [g], V. Wagner [p], C. Wendisch [d], J. Wirth [i,j], J. Wüstenfeld [f], Y. Zanevsky [g], P. Zumbruch [d]

[a] *Institute of Physics, Slovak Academy of Sciences, 84228 Bratislava, Slovakia*
[b] *LIP-Laboratório de Instrumentação e Física Experimental de Partículas, 3004-516 Coimbra, Portugal*
[c] *Smoluchowski Institute of Physics, Jagiellonian University of Cracow, 30-059 Kraków, Poland*
[d] *GSI Helmholtzzentrum für Schwerionenforschung GmbH, 64291 Darmstadt, Germany*
[e] *Technische Universität Darmstadt, 64289 Darmstadt, Germany*
[f] *Institut für Strahlenphysik, Helmholtz-Zentrum Dresden-Rossendorf, 01314 Dresden, Germany*
[g] *Joint Institute of Nuclear Research, 141980 Dubna, Russia*
[h] *Institut für Kernphysik, Goethe-Universität, 60438 Frankfurt, Germany*
[i] *Excellence Cluster 'Origin and Structure of the Universe', 85748 Garching, Germany*
[j] *Physik Department E62, Technische Universität München, 85748 Garching, Germany*
[k] *II.Physikalisches Institut, Justus Liebig Universität Giessen, 35392 Giessen, Germany*
[l] *Institute for Nuclear Research, Russian Academy of Science, 117312 Moscow, Russia*
[m] *Institute of Theoretical and Experimental Physics, 117218 Moscow, Russia*
[n] *Department of Physics, University of Cyprus, 1678 Nicosia, Cyprus*
[o] *Institut de Physique Nucléaire (UMR 8608), CNRS/IN2P3-Université Paris Sud, F-91406 Orsay Cedex, France*
[p] *Nuclear Physics Institute, Academy of Sciences of Czech Republic, 25068 Rez, Czech Republic*
[q] *LabCAF. F. Física, Univ. de Santiago de Compostela, 15706 Santiago de Compostela, Spain*

* Corresponding authors.
E-mail addresses: Laura.Fabbietti@ph.tum.de (L. Fabbietti), Tobias.Kunz@tum.de (T. Kunz).
[1] Also at ISEC Coimbra, Coimbra, Portugal.
[2] Also at ExtreMe Matter Institute EMMI, 64291 Darmstadt, Germany.
[3] Also at Technische Universität Dresden, 01062 Dresden, Germany.
[4] Also at Frederick University, 1036 Nicosia, Cyprus.
[5] Also at Dipartimento di Fisica and INFN, Università di Torino, 10125 Torino, Italy.

https://doi.org/10.1016/j.physletb.2018.02.043

ARTICLE INFO

Article history:
Received 15 November 2017
Received in revised form 17 February 2018
Accepted 19 February 2018
Available online 23 February 2018
Editor: D.F. Geesaman

Keywords:
Hyperons
Strangeness
Proton
Nucleus

ABSTRACT

The production of Σ^0 baryons in the nuclear reaction p (3.5 GeV) + Nb (corresponding to $\sqrt{s_{NN}} = 3.18$ GeV) is studied with the detector set-up HADES at GSI, Darmstadt. Σ^0s were identified via the decay $\Sigma^0 \to \Lambda\gamma$ with subsequent decays $\Lambda \to p\pi^-$ in coincidence with a e^+e^- pair from either external ($\gamma \to e^+e^-$) or internal (Dalitz decay $\gamma^* \to e^+e^-$) gamma conversions. The differential Σ^0 cross section integrated over the detector acceptance, i.e. the rapidity interval $0.5 < y < 1.1$, has been extracted as $\Delta\sigma_{\Sigma^0} = 2.3 \pm (0.2)^{stat} \pm \left(^{+0.6}_{-0.6}\right)^{sys} \pm (0.2)^{norm}$ mb, yielding the inclusive production cross section in full phase space $\sigma^{total}_{\Sigma^0} = 5.8 \pm (0.5)^{stat} \pm \left(^{+1.4}_{-1.4}\right)^{sys} \pm (0.6)^{norm} \pm (1.7)^{extrapol}$ mb by averaging over different extrapolation methods. The Λ_{all}/Σ^0 ratio within the HADES acceptance is equal to $2.3 \pm (0.2)^{stat} \pm (^{+0.6}_{-0.6})^{sys}$. The obtained rapidity and momentum distributions are compared to transport model calculations. The Σ^0 yield agrees with the statistical model of particle production in nuclear reactions.

1. Introduction

The study of hyperon production in proton-induced collisions at beam energies of a few GeV is important for many open questions in the field of hadron physics. While several experimental results exist for Λ hyperons in p+p and p+A reactions [1–6], measurements of Σ^0 production are scarce [4–6]. The dominant electromagnetic decay $\Sigma^0 \to \Lambda + \gamma$ (BR $\approx$ 100%) requires the identification of photons with $E_\gamma \simeq 80$ MeV coincident to the detection of $p\pi^-$ pairs from Λ decays. Our measurement is the first step towards gaining access to the hyperon electromagnetic form factors [7]. Once the measurement of virtual photons in the Dalitz decay $\Sigma^0 \to \Lambda e^+e^-$ (BR < 1%) is performed it can be separated from the decays involving a real photon and therefore provide complementary information on the nucleon and Δ baryon form factors [8].

Hadron collisions at energies of a few GeV with hyperons in the final state are also suited to study the role played by intermediate hadronic resonances in the strangeness production process. Indeed, non-strange resonances like N* and Δ have been found to contribute significantly [9–13] via the channels $N^* \to \Lambda + K^+$ and $\Delta^{++} \to \Sigma(1385)^+ + K^+$. In case of N*, up to seven resonances with similar masses and widths have been identified including the occurrence of interference effects among them [2,14]. In this context, the simultaneous measurement of Λ and Σ hyperons becomes important to understand the interplay between the spin 1/2 and 3/2 states occurring in the strong conversion process $\Sigma + N \to \Lambda + N$. This process manifests itself as a peak structure on top of the smooth $\Lambda + p$ invariant-mass distribution close to the Σ–N threshold and is known to be responsible for cusp effects [15]. Hyperon production in nuclear reactions gives also access to details of the hyperon–nucleon interaction. The existence of Λ hypernuclei is argued as evidence for an attractive potential at rather large inter-baryon distances [16,17]. Theoretical models [18] trying to describe scattering data [19,20] with hyperon beams postulate the presence of a repulsive core for the Λ–N interaction. Σ^0 hypernuclei, on the other hand, have not been observed so far due to difficulties implied by the electromagnetic Σ^0 decays and the requirement of large acceptance and high resolution electromagnetic calorimeters. Since also scattering data for Σ hyperon beams are scarce, constraints on the Σ–N interaction are missing so far and new measurements of Σ^0 production in nuclear targets are essential.

Medium-energy heavy-ion collisions producing hyperons allow to study their properties within a dense baryonic environment (up to $\rho \approx 2-3\rho_0$) [21–24]. One question of interest is whether the attractive Λ–N interaction in vacuum or at nuclear saturation might change due to the postulated appearance of a more dominant repulsive core at increased densities and short distances [25]. The quest for detailed information on such aspects requires the knowledge of Λ feed down effects from Σ^0 production and its corresponding behaviour in baryonic or even cold nuclear matter.

Experimental data for simultaneous Σ^0 and Λ production are available for proton–proton collisions either close to the free NN production threshold ($E_{th} = 2.518$ GeV for Λ and $E_{th} = 2.623$ GeV for Σ^0) [4,5] or at excess energies of $\simeq 5$ GeV and above [26]. So far, no data are available for Σ^0 hyperons emerging from proton + nucleus collision systems at few GeV incident beam energy. In this work we present the first measurement of Σ^0 production in p + Nb collisions at an incident kinetic beam energy of $E_p = 3.5$ GeV. Our paper is organised as follows. In section 2, we describe the experimental set-up. Section 3 is devoted to Σ^0 identification and background subtraction. In section 4 the method for efficiency correction and differential analysis is shown. In section 6 the extracted cross sections and yields are compared to different models. In sections 6 we give a summary and short outlook.

2. The HADES experiment

The High-Acceptance Di-Electron Spectrometer (HADES) [27] located at the GSI Helmholtzzentrum für Schwerionenforschung in Darmstadt (Germany) is an experimental facility for fixed target nuclear reaction studies in the few GeV energy region. The spectrometer is dedicated to measure low-mass dielectrons originating from the decay of vector mesons in the invariant-mass range up to the ϕ mass and offers excellent identification by means of charged hadrons such as pions, kaons and protons. The detector setup covers polar angles between 18° to 85° over almost the full azimuthal range designed to match the mid-rapidity region of symmetric heavy ion collisions at E = 1–2 AGeV. A set of multi-wire drift chamber (MDC) planes arranged in a sixfold segmented trapezoidal type structure, two layers in front and two behind a toroidal magnetic field, is used for charged-particle tracking and momentum reconstruction with a typical resolution of $\Delta p/p \simeq 3\%$. An electromagnetic shower detector (Pre-Shower) and a Time-Of-Flight scintillator wall (TOF and TOFINO) build the Multiplicity and Electron Trigger Array (META) detector system used for event trigger purposes. The energy loss (dE/dx) signals measured in the TOF and MDC detectors are used for charged particle identification. In addition, electrons and positrons are identified over a large range of momenta with a Ring Imaging Cherenkov (RICH) detector surrounding the target in a nearly field-free region.

In the present experiment, a proton beam accelerated by the SIS18 synchrotron to a kinetic energy of $E_p = 3.5$ GeV has been

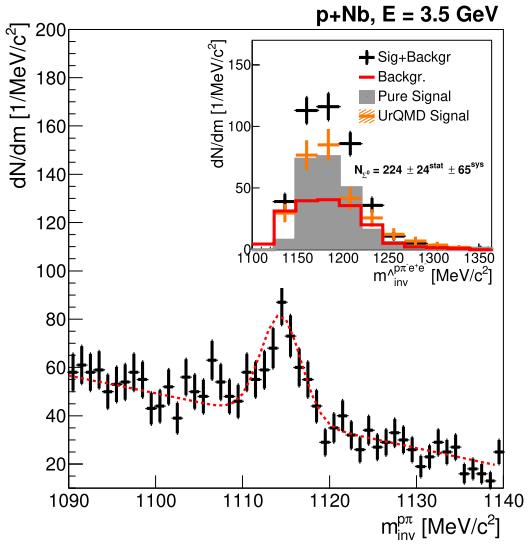

Fig. 1. (Colour online.) Invariant mass distribution of $p\pi^-$ pairs with an additional e^+–e^- pair in the same event. The dashed curve shows a combination of a polynomial background fit and a gaussian fit applied to the signal area. **Inset:** Four-particle invariant mass distribution of a proton, pion and dielectron for $p\pi^-$ pairs in the Λ signal region. Measured signal (black crosses), combinatorial background (red histogram) and extracted net signal (gray line) are shown in comparison to a UrQMD simulation (orange histogram) with scaled Σ^0 production.

directed on a twelve-fold segmented ^{93}Nb target of 2.8% nuclear interaction probability. For a TOF+TOFINO reaction trigger setting of multiplicity $M \geq 3$ and at typical beam intensities of 2×10^6 particles/s on target, a total of 3.2×10^9 events have been recorded and analysed.

3. Σ^0 identification and background subtraction

The identification of Σ^0 hyperons was achieved via the decay channel $\Sigma^0 \rightarrow \Lambda\gamma$ (BR $\approx$ 100% [28]) by reconstructing $\Lambda \rightarrow p\pi^-$ decays correlated with the emission of a dielectron from external pair conversion $\gamma \rightarrow e^+e^-$ or from the Dalitz decay $\Sigma^0 \rightarrow \Lambda e^+e^-$ (BR $< 5 \cdot 10^{-3}$ [28]). Fig. 1 depicts the $p\pi^-$ invariant-mass distribution of such events with a clear signature of a Λ content in the data sample. Due to the low mass difference $m_{\Sigma^0} - m_\Lambda \approx 77$ MeV/c^2 a considerable fraction of coincident $e^\pm$ candidates have momenta below the spectrometer acceptance threshold $p_{thr} \approx 50$ MeV/c needed for full track and momentum reconstruction. For this reason, dielectrons have been identified by requiring two RICH rings, at least one fully reconstructed $e^\pm$ track and one neighbouring incomplete tracklet detected in front of the magnetic field in the first two MDCs. The missing momentum of the incomplete tracklet has been estimated by applying a most probable hypothesis as described in detail in [29] which partly exploits results and constraints from kinematically similar π^0 Dalitz decays. In this way, the observed incomplete dielectrons are combined into most probable photon signals with a resolution of δE_γ (FWHM) = 57 ± 2 MeV [29].

The combinatorial background has been determined with two approaches. First, background yield and shape have been estimated from polynomial fits of the $p\pi^-$ invariant mass in the sideband regions below and above the Λ peak, 1090 MeV/c^2 < $m_{inv}^{p\pi^-}$ < 1105 MeV/c^2 and 1125 MeV/c^2 < $m_{inv}^{p\pi^-}$ < 1140 MeV/c^2 (see Fig. 1). The second approach aimed at the suppression of a random peak structure. The momentum of the proton and pion was smeared by 2% such that the resulting invariant mass of proton and pion did not show any Λ peak. The obtained distribution was scaled to the sideband of the unsmeared distribution shown in Fig. 1 to evaluate the background in the signal region. After weighting and normalisation, both methods lead to the same background yield within 10%. The side band samples used to construct the $p\pi^-$ background are combined with the reconstructed $e^\pm$ pairs to obtain the background to the Σ^0 candidates (for details see [29]).

The inclusive four-particle $p\pi^-e^\pm$ invariant mass distribution is shown in the inset of Fig. 1. A peak structure becomes apparent at the Σ^0 pole mass with a width (FWHM) of 52 ± 22 MeV/c^2. The observed FWHM is mainly attributed to the resolution of the γ reconstruction. The estimated background is shown by the red histogram.

Full scale UrQMD [30,31] simulations have been carried out and processed through Geant and a digitisation procedure to emulate the detector response. Subsequently the events have then been analysed in the same manner as the experimental data. Then the simulation has been normalised to the Σ^0 yield. The inset in Fig. 1 shows that the simulated Σ^0 mass distribution is in agreement with the measured distribution. A total of $N_{\Sigma^0} = 224 \pm 24^{stat} \pm 65^{sys}$ Σ^0 candidates has been extracted.

4. Efficiency correction and differential analysis

After background subtraction, a differential analysis has been performed for the kinematic variables transverse momentum p_t and rapidity y of the Σ^0 candidates. Due to the limited event statistics, the experimental yields are computed for three equally spaced momentum bins between 240 MeV/c $\leq p_t \leq$ 960 MeV/c split in two rapidity bins $0.5 < y < 0.8$ and $0.8 < y < 1.1$. The acceptance and efficiency correction matrix for this phase space region has been obtained from simulations utilizing the UrQMD/Geant3 data set (see above) before and after Σ^0 reconstruction. The systematic errors of these corrections stem from various sources. The uncertainty on particle identification of protons and pions of $\simeq 5\%$ is adopted from the high statistics analysis of inclusive Λ production [3]. The overall uncertainty for identification of low momentum e^+/e^- partners and pair reconstruction with two complete tracks is $\simeq 25\%$ as deduced in a previous search for dark photons with hypothetical masses in the interval $\simeq$ 50–100 MeV [32]. The error in the background subtraction is estimated from a comparison of the two methods described above and contributes with $\simeq 8\%$. Other sources are of order 10^{-2} and less. The quadratic sum results in a total systematic error of $\approx 30\%$. The statistical errors did not exceed values of $\simeq$ 10–30%.

The corrected reduced transverse-mass spectra (with $m_t = \sqrt{p_t^2 + m_{\Sigma^0}^2}$) for the Σ^0 candidates are shown in Fig. 2 separately for both rapidity intervals. Towards smaller transverse momenta, the geometrical spectrometer acceptance does not cover the full region for at least one of the decay partners Λ or γ. To extrapolate to uncovered phase space regions we have assumed a thermal Σ^0 phase space production. Hence, the differential distributions have been fitted with a Maxwell–Boltzmann distribution $(1/m_t^2)(d^2N/(dm_t dy)) = A(y) \cdot \exp(-((m_t - m_{\Sigma^0})c^2)/(T_B(y))$, where $A(y)$ is a rapidity dependent scaling factor and $m_{\Sigma^0} = 1192.642 \pm 0.024$ MeV/c^2 [28]. The inverse-slope parameters $T_B = 82 \pm 23$ MeV for the rapidity bin $0.5 < y < 0.8$ and $T_B = 78 \pm 22$ MeV for the more forward region $0.8 < y < 1.1$ can be compared with the average value of 84 MeV extracted for Λ hyperons in the same reaction [3].

The experimental rapidity–density distributions dN/dy obtained for both hyperons from integration of the corresponding Maxwell–Boltzmann distributions with the given parameters are depicted in the upper panel of Fig. 3. The calculation of minimum-bias multiplicities requires normalisation of the observed yields to the

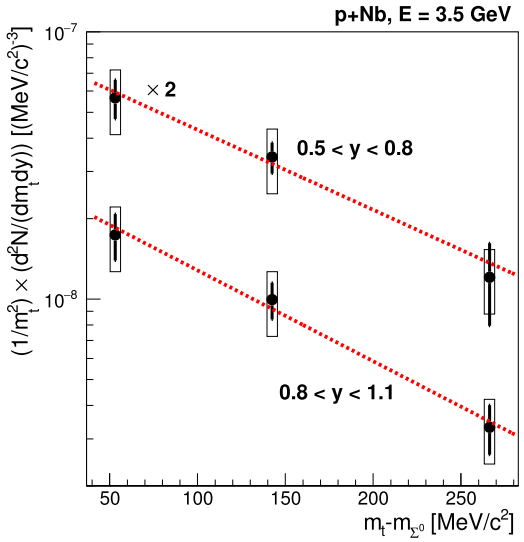

Fig. 2. (Colour online.) Reduced transverse mass distributions of Σ^0s corrected for acceptance and detection efficiency. The data are plotted for two rapidity bins. The red dashed lines indicate Maxwell–Boltzmann fits. See text for details.

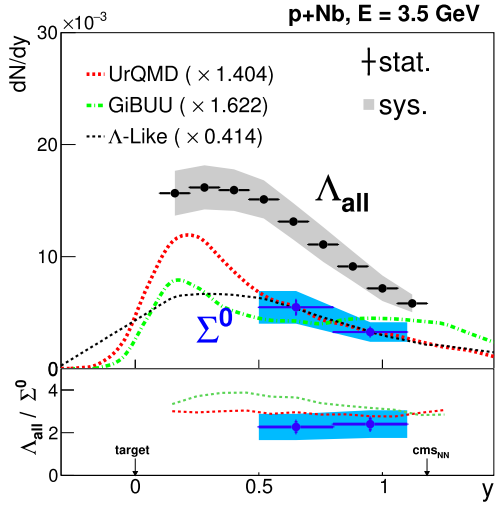

Fig. 3. (Colour online.) **Top:** Experimental rapidity–density distributions of Λ (black) and Σ^0 (blue) hyperons. The Λ distribution [3] refers to all experimentally identified Λs. The shaded bands denote the systematic errors. The dotted lines represent model calculations scaled to match the measured Σ^0 yield (see text). **Bottom:** The unscaled ratio Λ_{all}/Σ^0. Colour and line codes as in top panel.

total number of reactions which we obtained by multiplying the number of M3 triggers (charged particle multiplicity ≥ 3) with a correction factor C. The latter has been extracted from a UrQMD simulation of the p+Nb reaction with impact parameters in the range 0–8 fm and full Geant3 propagation of the events yielding $C = 1/R^{M3\to M1}_{Trigger}$ with $R^{M3\to M1}_{Trigger} = 0.58 \pm 0.06$. Summation over both rapidity bins in Fig. 3 gives the multiplicity inside the acceptance $N_{\Sigma^0} = (2.7 \pm (0.2)^{stat} \pm \left(^{+0.7}_{-0.7}\right)^{sys} \pm (0.2)^{norm}) \times 10^{-3}$/evt. and $N_{\Lambda_{all}} = (6.1 \pm (^{+0.3}_{-0.3})^{sys} \pm (0.8)^{norm} \times 10^{-3}$/evt. Note that the $N_{\Lambda_{all}}$ signal includes the feed down from heavier resonances, mainly from Σ^0 decays. The production ratio inside the acceptance $0.5 < y < 1.1$ is found to be $\Lambda_{all}/\Sigma^0 = 2.3 \pm (0.2)^{stat} \pm \left(^{+0.6}_{-0.6}\right)^{sys}$.

Table 1
Total Σ^0 yields and cross sections after extrapolation under three assumptions.

Shape	Σ^0 yield per event	$\sigma^{total}_{\Sigma^0}$ [mb]
Λ-like	5.2×10^{-3}	$4.4 \pm 0.4^{stat} \pm 1.1^{sys} \pm 0.5^{norm}$
GiBUU	7.3×10^{-3}	$6.2 \pm 0.5^{stat} \pm 1.5^{sys} \pm 0.6^{norm}$
UrQMD	8.6×10^{-3}	$7.3 \pm 0.6^{stat} \pm 1.8^{sys} \pm 0.8^{norm}$

5. Cross sections and comparison to models

The production cross section has then been obtained by multiplying the multiplicity with the total interaction cross section $\sigma_{pNb} = 848 \pm 126$ mb for the p + Nb reaction [33,34] and correcting it for the trigger bias. The acceptance integrated cross section $\Delta\sigma_{\Sigma^0}$ which can be obtained from the experimental count rates by multiplication with the luminosity is found to be equal to $\Delta\sigma_{\Sigma^0} = 2.3 \pm (0.2)^{stat} \pm \left(^{+0.6}_{-0.6}\right)^{sys} \pm (0.2)^{norm}$ mb within the rapidity interval $0.5 < y < 1.1$.

Extrapolation to the uncovered rapidity region and extraction of an estimate for the total production cross section have been deduced with the help of transport model calculations. We have extracted Σ^0 rapidity distributions from UrQMD [30] and GiBUU [35,36] event generators and normalised them to match the experimental data points. The distributions are plotted in Fig. 3 and exhibit considerable differences. Those possibly indicate different weights in the models for the implementation of the slowing down of the Σ^0 which are initially produced at the rapidity of the NN centre-of-mass system. While the data are well reproduced by UrQMD in the region above $y > 0.4$, the extrapolation to target rapidities seems to be ambiguous. Under the assumption that both hyperons experience comparable emission kinematics due to their very similar masses we can profit from the larger rapidity coverage and smaller bin sizes of the reconstructed Λ. Hence, as an alternative guidance we have used the measured Λ rapidity density distribution (Λ-like) as published in [3] and normalised it to the Σ^0 distribution. For comparison, the resulting total Σ^0 yields and extrapolated production cross sections of the scaled distributions are listed in Table 1.

The Σ^0 production cross section has finally been calculated from a mean of the Λ-like and UrQMD rapidity distributions resulting in $\sigma^{tot}_{p+Nb}(\Sigma^0) = 5.8 \pm (0.5)^{stat} \pm \left(^{+1.4}_{-1.4}\right)^{sys} \pm (0.6)^{norm} \pm (1.7)^{extrapol}$ mb. A Σ^0 yield of $N_{\Sigma^0} = (7 \pm 3) \times 10^{-3}$/evt for the full phase space has been extracted in the same way. The ratio $\Lambda_{all}/\Sigma^0 = 2.3 \pm (0.2)^{stat} \pm (^{+0.7}_{-0.7})^{sys} \pm (0.7)^{extrapol}$ has been obtained by using the ratio within the acceptance and an additional extrapolation uncertainty stemming from the difference between UrQMD and Λ-like extrapolation methods. This can be justified by the rather flat distribution of experimental data as well as for the UrQMD and GiBUU simulations. The error on the extrapolation procedure introduces the largest uncertainty. The statistical and systematic errors have been added quadratically. Fig. 4 shows our result for the total number (i.e., full phase space extrapolated) of Λs not stemming from Σ^0 decays (that is the number of identified Λs minus the number of Λs identified as decay products of Σ^0s) divided by the number of Σ^0s, $R = 1.3 \pm 0.6$, together with a compilation of the world data [4–6,26,37] and a data fit [37] plotted as a function of excess energy above the nucleon–nucleon threshold. The results from UrQMD are shown for comparison. All data points but two stem from proton–proton collisions. Our result for the production in a heavy nucleus (heavy bullet in Fig. 4) fits well to the systematics and model predictions. In this comparison, the multi-step interaction of the Σ^0 with one, two or even more nucleons has been neglected as well as the Fermi motion.

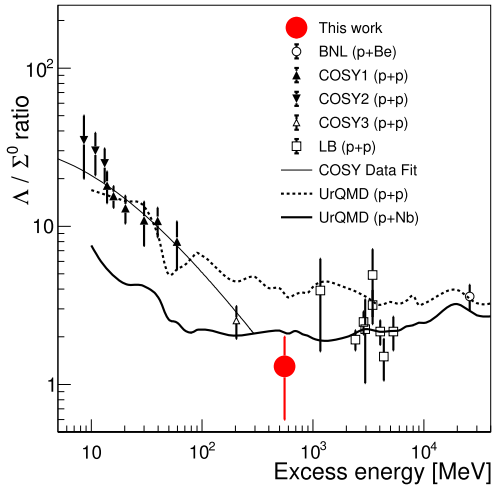

Fig. 4. (Colour online.) Experimental excitation function of Λ/Σ^0 production cross section ratios from exclusive measurements of $\sigma(pp \to pK\Lambda)$ and $\sigma(pp \to pK\Sigma^0)$ reactions. The excess energy above production threshold refers to free nucleon–nucleon collisions. Data (symbols) from BNL [6], COSY [4,5,37], LB [26] and present work. The thin curve is a fit from [37]. The dotted and solid curves exhibit UrQMD simulations. Fermi motion has been neglected for p+A collisions.

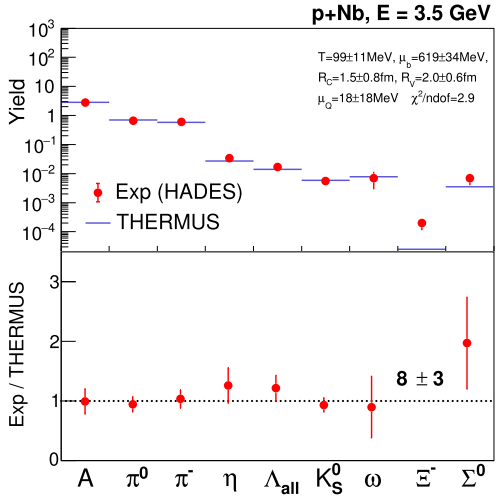

Fig. 5. (Colour online.) Experimental hadron yields measured by HADES [39] in comparison to a THERMUS statistical model fit w/o Σ^0.

We now compare our findings to the statistical model THERMUS [38]. In this model, the total particle abundances strictly follow a distribution expected from hadron freeze-out at conditions determined by a temperature $T_{f.o.}$ and a baryochemical potential $\mu_{f.o.}$. For this scenario, particle yields are proportional to $e^{(E-\mu_{f.o.})/T_{f.o.}}$. A THERMUS fit to measured particle yields [39], excluding the Σ^0, gives parameter values $T_{f.o.} = 100$ MeV and $\mu_{f.o.} = 620$ MeV. For these parameters (see legend in Fig. 5), the expected Σ^0 yield slightly underestimates (1.5 σ) the inclusive experimental value presented in this work. Fig. 5 shows the corresponding THERMUS fit results. The THERMUS yield ratio $\Lambda_{all}/\Sigma^0 = 3.9$ is slightly higher than that predicted by GiBUU, UrQMD ($R \simeq 3$) and our measurement ($R \simeq 2.3$). Nevertheless, the overall agreement is surprising for proton induced nuclear collisions at relatively low energies, as already discussed in [39].

6. Summary and outlook

We have demonstrated the capability of HADES to reconstruct the low energy $\gamma \to e^+e^-$ conversion processes in the detector material via the identification of electrons and positrons. With this technique we were able to measure for the first time Σ^0 hyperon production in proton-induced reactions off a heavy nucleus near threshold. We provide transverse mass distributions in two rapidity bins. Based on them, a Σ^0 production cross section of $\sigma_{p+Nb}(\Sigma^0) = 5.8 \pm 2.3$ mb has been determined. The inclusive light hyperon production ratio is $\Lambda_{all}/\Sigma^0 = 2.3 \pm 1.1$. All uncertainties have been summed up quadratically. These experimental values compare reasonably well with transport model calculations and results from a statistical hadronisation scheme. In spite of the limited spectrometer acceptance the obtained relative production cross sections may hint to a slightly larger production probability in nuclei as compared to expectations from proton–proton collisions, $\frac{\Sigma^0}{\Lambda}|_{pA} > \frac{\Sigma^0}{\Lambda}|_{pp}$. A possible measurement with a low magnetic field will allow full reconstruction of the dielectrons and therefore offer the possibility to determine electromagnetic transition formfactors. The currently ongoing upgrade includes an electromagnetic calorimeter which will significantly enhance the γ detection capabilities of HADES. Measurements able to separate the contribution of p–p and p–n reactions are planned, which go beyond the average values extracted now from proton-nucleus collisions. This opens up the investigation of reaction channels involving photon decays of hyperons and other baryonic resonances produced in proton/pion–proton, proton/pion-nucleus and heavy-ion collisions and might even give access to measurements of electromagnetic transition form factors for these resonances.

Acknowledgements

The HADES collaboration gratefully acknowledges the support by the grants VH-NG-823, TU Darmstadt (Germany); BMBF05P15WOFCA, DFG EClust 153, MLL, TU München (Germany); BMBF05P12RGGHM, JLU Giessen (Germany); CNRS/IN2P3, IPN Orsay (France); GACR13-06759S, MSMT LM2015049, Rez (Czech Republic); BMBF05P15PXFCA, GSI WKAMPE1416, BU Wuppertal (Germany); NCN 2013/10/M/ST2/00042 (Poland); NSC 2016/23/P/ST2/04066 POLONEZ (Poland).

References

[1] J. Adamczewski-Musch, et al., Inclusive Λ production in proton–proton collisions at 3.5 GeV, Phys. Rev. C 95 (1) (2017) 015207, https://doi.org/10.1103/PhysRevC.95.015207.
[2] R. Münzer, et al., Determination of N* amplitudes from associated strangeness production in p + p collisions, arXiv:1703.01978.
[3] G. Agakishiev, et al., Lambda hyperon production and polarization in collisions of p(3.5 GeV)+Nb, Eur. Phys. J. A 50 (2014) 81, https://doi.org/10.1140/epja/i2014-14081-2.
[4] P. Kowina, et al., Energy dependence of the Λ/Σ^0 production cross-section ratio in p–p interactions, Eur. Phys. J. A 22 (2) (2004) 293–299.
[5] S. Sewerin, et al., Comparison of Λ and Σ^0 threshold production in proton–proton collisions, Phys. Rev. Lett. 83 (1999) 682–685, https://doi.org/10.1103/PhysRevLett.83.682.
[6] M.W. Sullivan, et al., Measurement of the ratio of Σ^0 to Λ^0 inclusive production from 28.5-GeV/c protons on beryllium, Phys. Rev. D 36 (1987) 674, https://doi.org/10.1103/PhysRevD.36.674.
[7] C. Granados, S. Leupold, E. Perotti, The electromagnetic Sigma-to-Lambda hyperon transition form factors at low energies, Eur. Phys. J. A 53 (6) (2017) 117, https://doi.org/10.1140/epja/i2017-12324-4.
[8] J. Adamczewski-Musch, et al., Δ(1232) Dalitz decay in proton–proton collisions at T=1.25 GeV measured with HADES at GSI, Phys. Rev. C 95 (6) (2017) 065205, https://doi.org/10.1103/PhysRevC.95.065205.
[9] S. Abdel-Samad, et al., Hyperon production in the channel pp→p$K^+\Lambda$ near the reaction threshold, Phys. Lett. B 632 (2006) 27–34, https://doi.org/10.1016/j.physletb.2005.09.086.

[10] M. Röder, et al., Final-state interactions in the process $\vec{p}p \to pK^+\Lambda$, Eur. Phys. J. A 49 (2013) 157, https://doi.org/10.1140/epja/i2013-13157-9.

[11] R. Siebert, et al., High resolution study of hyperon nucleon interactions by associated strangeness production in pp collisions, Nucl. Phys. A 567 (1994) 819–843, https://doi.org/10.1016/0375-9474(94)90329-8.

[12] F. Hauenstein, et al., First model-independent measurement of the spin triplet $p\Lambda$ scattering length from final state interaction in the $\vec{p}p \to pK^+\Lambda$ reaction, Phys. Rev. C 95 (3) (2017) 034001, https://doi.org/10.1103/PhysRevC.95.034001.

[13] G. Agakishiev, et al., Baryonic resonances close to the $\bar{K}$ N threshold: the case of $\Sigma(1385)^+$ in pp collisions, Phys. Rev. C 85 (2012) 035203, https://doi.org/10.1103/PhysRevC.85.035203.

[14] G. Agakishiev, et al., Partial wave analysis of the reaction $p(3.5\ \mathrm{GeV}) + p \to pK^+\Lambda$ to search for the "ppK^-" bound state, Phys. Lett. B 742 (2015) 242–248, https://doi.org/10.1016/j.physletb.2015.01.032.

[15] S. Abd El-Samad, E. Borodina, K.T. Brinkmann, H. Clement, E. Doroshkevich, et al., On the ΣN cusp in the pp→pK$^+\Lambda$ reaction, Eur. Phys. J. A 49 (2013) 41, https://doi.org/10.1140/epja/i2013-13041-8.

[16] A. Feliciello, T. Nagae, Experimental review of hypernuclear physics: recent achievements and future perspectives, Rep. Prog. Phys. 78 (9) (2015) 096301, https://doi.org/10.1088/0034-4885/78/9/096301.

[17] A. Gal, E.V. Hungerford, D.J. Millener, Strangeness in nuclear physics, Rev. Mod. Phys. 88 (3) (2016) 035004, https://doi.org/10.1103/RevModPhys.88.035004.

[18] J. Haidenbauer, S. Petschauer, N. Kaiser, U.G. Meissner, A. Nogga, W. Weise, Hyperon–nucleon interaction at next-to-leading order in chiral effective field theory, Nucl. Phys. A 915 (2013) 24–58, https://doi.org/10.1016/j.nuclphysa.2013.06.008.

[19] B. Sechi-Zorn, B. Kehoe, J. Twitty, R.A. Burnstein, Low-energy lambda-proton elastic scattering, Phys. Rev. 175 (1968) 1735–1740, https://doi.org/10.1103/PhysRev.175.1735.

[20] F. Eisele, H. Filthuth, W. Föhlisch, V. Hepp, G. Zech, Elastic sigma+- p scattering at low energies, Phys. Lett. B 37 (1971) 204–206, https://doi.org/10.1016/0370-2693(71)90053-0.

[21] N. Bastid, et al., K0 and Lambda production in Ni + Ni collisions near threshold, Phys. Rev. C 76 (2007) 024906, https://doi.org/10.1103/PhysRevC.76.024906.

[22] G. Agakishiev, et al., Hyperon production in Ar+KCl collisions at 1.76A GeV, Eur. Phys. J. A 47 (2011) 21, https://doi.org/10.1140/epja/i2011-11021-8.

[23] C. Pinkenburg, et al., Production and collective behavior of strange particles in Au + Au collisions at 2-AGeV–8-AGeV, Nucl. Phys. A 698 (2002) 495–498, https://doi.org/10.1016/S0375-9474(01)01412-9.

[24] P. Chung, et al., Directed flow of Lambda hyperons in 2-AGeV to 6-AGeV Au+Au collisions, Phys. Rev. Lett. 86 (2001) 2533–2536, https://doi.org/10.1103/PhysRevLett.86.2533.

[25] S. Petschauer, J. Haidenbauer, N. Kaiser, U.-G. Meißner, W. Weise, Hyperons in nuclear matter from SU(3) chiral effective field theory, Eur. Phys. J. A 52 (1) (2016) 15, https://doi.org/10.1140/epja/i2016-16015-4.

[26] A. Baldini, Numerical Data and Functional Relationships in Science and Technology, Landolt-Boernstein, New Series 1/128, vol. 12, Springer Verlag, 1988.

[27] G. Agakishiev, et al., The high-acceptance dielectron spectrometer HADES, Eur. Phys. J. A 41 (2009) 243–277, https://doi.org/10.1140/epja/i2009-10807-5.

[28] C. Patrignani, et al., Review of particle physics, Chin. Phys. C 40 (10) (2016) 100001, https://doi.org/10.1088/1674-1137/40/10/100001.

[29] T. Kunz, et al., Σ^0 identification in proton induced reactions on a nuclear target, in: Proceeding Bormio 55th Wintermeeting on Nuclear Physics, 2017.

[30] S.A. Bass, et al., Microscopic models for ultrarelativistic heavy ion collisions, Prog. Part. Nucl. Phys. 41 (1998) 255–369, https://doi.org/10.1016/S0146-6410(98)00058-1, Prog. Part. Nucl. Phys. 41 (1998) 225.

[31] Urqmd version 3.4, http://urqmd.org/documentation/urqmd-3.4.pdf.

[32] G. Agakishiev, et al., Searching a dark photon with HADES, Phys. Lett. B 731 (2014) 265–271, https://doi.org/10.1016/j/physletb.2014.02.035.

[33] G. Agakishiev, et al., Inclusive pion and η production in p+Nb collisions at 3.5 GeV beam energy, Phys. Rev. C 88 (2) (2013) 024904, https://doi.org/10.1103/PhysRevC.88.024904.

[34] G. Agakishiev, et al., First measurement of proton-induced low-momentum dielectron radiation off cold nuclear matter, Phys. Lett. B 715 (2012) 304–309, https://doi.org/10.1016/j.physletb.2012.08.004.

[35] G.F. Bertsch, H. Kruse, S.D. Gupta, Boltzmann equation for heavy ion collisions, Phys. Rev. C 29 (1984) 673–675, https://doi.org/10.1103/PhysRevC.29.673, Erratum: Phys. Rev. C 33 (1986) 1107, https://doi.org/10.1103/PhysRevC.33.1107.

[36] Gibuu version 2016, https://gibuu.hepforge.org/documentation2016/.

[37] M. Abdel-Bary, et al., Production of Λ and Σ^0 hyperons in proton–proton collisions, Eur. Phys. J. A 46 (2010) 27–44, https://doi.org/10.1140/epja/i2010-11023-0, Erratum: Eur. Phys. J. A 46 (2010) 435, https://doi.org/10.1140/epja/i2010-11062-5.

[38] S. Wheaton, J. Cleymans, THERMUS: a thermal model package for ROOT, Comput. Phys. Commun. 180 (2009) 84–106, https://doi.org/10.1016/j.cpc.2008.08.001.

[39] G. Agakishiev, et al., Statistical hadronization model analysis of hadron yields in p + Nb and Ar + KCl at SIS18 energies, Eur. Phys. J. A 52 (6) (2016) 178, https://doi.org/10.1140/epja/i2016-16178-x.